Hindawi
Mathematical Problems in Engineering
Volume 2018, Article ID 2869731, 7 pages
https://doi.org/10.1155/2018/2869731

Research Article

Modulation of Pulse Train Using Leapfrogging Pulses Developed in Unbalanced Coupled Nonlinear Transmission Lines

Koichi Narahara

Department of Electrical and Electronic Engineering, Kanagawa Institute of Technology, 1030 Shimoogino, Atsugi, Kanagawa 243-0292, Japan

Correspondence should be addressed to Koichi Narahara; narahara@ele.kanagawa-it.ac.jp

Received 18 October 2017; Accepted 14 January 2018; Published 12 February 2018

Academic Editor: Ben T. Nohara

The leapfrogging pulses in two unbalanced electrical nonlinear transmission lines (NLTLs) with capacitive couplings are investigated for efficient modulation of a pulse train. Due to the resonant interactions, the nonlinear solitary waves in the NLTLs exhibit complementary behaviors of amplitudes and phases called leapfrogging. For maximizing resonance, both solitary waves should have a common average velocity. Sharing the common velocity, the characteristic impedance can still be freely designed for two coupled solitary waves. In this study, we characterize the leapfrogging pulses developed in unbalanced NLTLs having distinct characteristic impedance. Through the soliton perturbation theory and numerical time-domain calculations, it is found that both the leapfrogging frequency and the voltage variations of pulse amplitudes increase as the difference in the characteristic impedance becomes large. These properties can improve the on/off ratio of modulated pulse train.

1. Introduction

In coupled nonlinear systems, the resonant energy exchange can occur between supported nonlinear solitary waves. Through the energy transfer from the leading solitary wave to the trailing one, the leading wave is attenuated, whereas the amplitude of the trailing wave becomes larger than that of the leading wave. In weakly dispersive cases, the velocity of a long-wavelength nonlinear solitary wave increases as its amplitude increases; therefore, the trailing wave overtakes the leading wave. Then, the direction of energy transfer is reversed so that the original order of the two waves is restored. This overtaking is repeated, resulting in oscillatory behavior called leapfrogging [1]. Leapfrogging solitary waves have mainly been investigated on separated pycnoclines [2–6]. When two horizontal pycnoclines are vertically separated by a small amount, leapfrogging occurs between spatially localized disturbances in two pycnoclines. For weak couplings, the leapfrogging solitary waves are well modeled by the coupled Korteweg-de Vries (KdV) equations. Recently, we investigated two identical transmission lines with regularly spaced Schottky varactors coupled via capacitors, called coupled nonlinear transmission lines (NLTLs), and successfully observed leapfrogging phenomena for the nonlinear solitary waves developed in them [7]. Because of easiness in designing both nonlinearity and dispersion separately, the electronic system can characterize leapfrogging waves efficiently.

In addition, leapfrogging can be used to manage traveling electrical pulses. Originally, NLTLs have been used in ultrafast electronic circuits such as a subpicosecond electrical shock generator and a short-pulse amplifier [8–10]. For example, the leapfrogging can be used for the detection of temporal separation between two short pulses inputted to coupled NLTLs. It has been shown that leapfrogging pulses with relatively large amplitudes exhibit nontrivial properties as their initial relative delay varies. The phase and amplitude of leapfrogging pulses depend on the initial delay between incident pulses, such that the pulse amplitude at the output port varies with the initial delay. Accordingly, the temporal delay between two inputted pulses is converted to the pulse amplitude at the output [7]. Another potential of electrical leapfrogging pulses results from their management by the biasing voltage to the varactors. The leapfrogging frequency depends on the biasing voltage, so that the line length required for the pulses on the lines to become maximal also depends on the biasing voltage. Conversely, the pulse

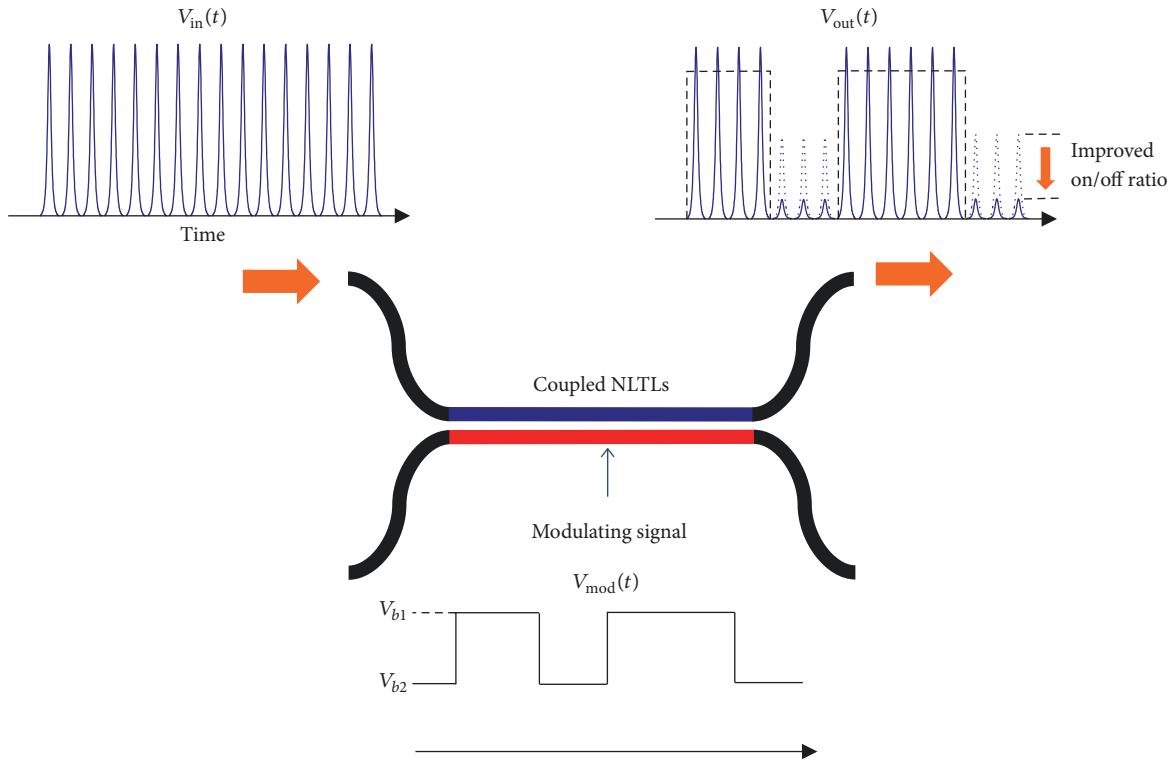

FIGURE 1: Modulation of pulse train using leapfrogging pulses in coupled NLTLs. The performance is considered better when V_{out} exhibits larger on/off ratio for smaller $|V_{b1} - V_{b2}|$.

amplitude on one of the lines can be managed by the biasing voltage at outputs that are separated from the inputs by a fixed length. The major output is thus switched from one line to the other by varying the bias voltage. Hence, the leapfrogging in coupled NLTLs can provide a novel switching method for the incident pulse by which the incident pulse is selectively output to one of the two ports of the coupled NLTLs [7]. The same mechanism can be used to modulate the inputted pulse train by the biasing voltage. Figure 1 illustrates this. The pulse train V_{in} inputted to the lines is modulated by V_{mod} to be outputted as V_{out}. In order to obtain fine modulation efficiency, the modulating signal is applied, such that the pulse amplitude at the output becomes maximal at $V_{mod} = V_{b1}$ and it becomes minimal at $V_{mod} = V_{b2}$. The on/off ratio of V_{out} is uniquely determined by the leapfrogging-pulse dynamics and can become larger than $|V_{b1} - V_{b2}|$. This means that only small swing of V_{mod} can give sufficient modulation. Including these examples, the key is to maximize the amplitude variation of the leapfrogging pulse.

Necessarily, the pulse wave in each line should have a common average velocity for securing sufficient interaction length. An electrical wave in an NLTL is uniquely determined only when both the velocity and characteristic impedance are specified. Even for the fixed velocity, the leapfrogging pulses still have the freedom to have their own characteristic impedance. In order to examine the potential for improving the extinction ratio of leapfrogging amplitudes, we consider the unbalanced NLTLs, where two leapfrogging pulses have the coincident velocity but distinct characteristic impedance.

After defining the imbalance, the coupled KdV equations with linear and dispersion-free coupling terms are derived to model the coupled NLTLs by applying the standard reductive perturbation method [11] to the transmission equations. Using this model, we clarify how imbalance improves the extinction ratio with the aid of the perturbation theory based on the inverse scattering transform [12–14]. We then validate the obtained results using time-domain calculations and demonstrate the performance of the coupled NLTLs as the pulse train modulator.

2. Fundamental Properties of Unbalanced Coupled NLTLs

Figure 2 shows the coupled NLTLs that we investigated. Lines 1 and 2 are weakly coupled via capacitors with a capacitance of C_m. The line inductance of line i is denoted as L_i for $i = 1, 2$. The Schottky varactors, the capacitance of which depends on the terminal voltage, are modeled by

$$C_{s1}(x) = C_1 \left(1 + \frac{V_b}{V_J}\right)^m \left(1 - \frac{x}{V_J}\right)^{-m},$$
$$C_{s2}(x) = C_2 \left(1 + \frac{W_b}{V_J}\right)^m \left(1 + \frac{x}{V_J}\right)^{-m}. \quad (1)$$

In this model, $C_{1,2}$, V_J, and m represent the junction capacitance for biasing voltages $-V_b$, W_b, junction potential, and grading coefficient, respectively. We consider the case

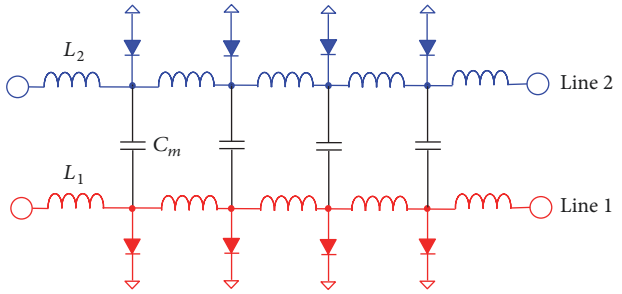

FIGURE 2: The structure of coupled NLTLs. Two NLTLs denoted as lines 1 and 2 are coupled with capacitors having the capacitance of C_m.

when line 1 is connected with loaded Schottky diode anodes and line 2 is connected with cathodes. Then, the transmission equations of the coupled NLTL are given by

$$\begin{aligned} L_1 \frac{dI_n}{dt} &= V_{n-1} - V_n, \\ L_2 \frac{dJ_n}{dt} &= W_{n-1} - W_n, \\ C_{s1}(V_n)\frac{dV_n}{dt} + C_m \frac{d}{dt}(V_n - W_n) &= I_n - I_{n+1}, \\ C_{s2}(W_n)\frac{dW_n}{dt} + C_m \frac{d}{dt}(W_n - V_n) &= J_n - J_{n+1}, \end{aligned} \tag{2}$$

where $V_n(W_n)$ and $I_n(J_n)$ represent the line voltage and current, respectively, at the nth cell of line 1 (line 2). Because KdV solitons are long waves, we apply the long-wavelength approximation to the transmission equations. A continuous spatial coordinate, x, is introduced by the relation

$$\begin{aligned} V_{n+1} &= V_n + \frac{\partial V}{\partial x} + \frac{1}{2}\frac{\partial^2 V}{\partial x^2} + \frac{1}{6}\frac{\partial^3 V}{\partial x^3} + \frac{1}{24}\frac{\partial^4 V}{\partial x^4}, \\ W_{n+1} &= W_n + \frac{\partial W}{\partial x} + \frac{1}{2}\frac{\partial^2 W}{\partial x^2} + \frac{1}{6}\frac{\partial^3 W}{\partial x^3} + \frac{1}{24}\frac{\partial^4 W}{\partial x^4}, \end{aligned} \tag{3}$$

where $V = V(x,t)$ and $W = W(x,t)$ are the continuous counterparts of V_n and W_n, respectively. From (2), we then obtain

$$\begin{aligned} &\{C_{s1}(V) + C_m\}\partial_t^2 V - C_m \partial_t^2 W + \frac{dC_{s1}(V)}{dV}(\partial_t V)^2 \\ &\quad = L_1^{-1}\left(\partial_x^2 V + \frac{1}{12}\partial_x^4 V\right), \\ &\{C_{s2}(W) + C_m\}\partial_t^2 W - C_m \partial_t^2 V + \frac{dC_{s2}(W)}{dW}(\partial_t W)^2 \\ &\quad = L_2^{-1}\left(\partial_x^2 W + \frac{1}{12}\partial_x^4 W\right), \end{aligned} \tag{4}$$

where $\partial_z = \partial/\partial z$ for any z. To derive coupled KdV equations modeling coupled NLTLs, we apply the reductive perturbation method [11]. Initially, new spatial and temporal variables, ξ and τ, respectively, are introduced according to

$$\xi = \epsilon^{1/2}\left(x - \frac{t}{\sqrt{C_1 L_1}}\right), \quad \tau = \epsilon^{3/2} t. \tag{5}$$

We then expand V and W in the series of ϵ as

$$\begin{aligned} V(\xi,\tau) &= -V_b + \sum_{i=1}^{\infty} \epsilon^i v^{(i)}(\xi,\tau), \\ W(\xi,\tau) &= W_b + \sum_{i=1}^{\infty} \epsilon^i w^{(i)}(\xi,\tau). \end{aligned} \tag{6}$$

Furthermore, C_m must be ϵ order quantity for the coupled KdV equations to be valid to model the coupled NLTL, such that we set

$$C_m = \epsilon C_m'. \tag{7}$$

Under this assumption, the velocity and characteristic impedance of the pulse on line i are estimated as $1/\sqrt{L_i C_i}$ and $\sqrt{L_i/C_i}$ $(i = 1, 2)$, respectively; therefore, the condition $L_1 C_1 = L_2 C_2$ is required to establish the significant resonant interactions between pulses on lines 1 and 2 and imbalance is introduced by setting $L_1/C_1 \neq L_2/C_2$. Substituting (5) and (6) into (4), we obtain the following coupled KdV equations with the conditions where the $O(\epsilon^3)$ terms disappear:

$$\begin{aligned} \partial_{\tau'} v' - 6v'\partial_{\xi'} v' + \partial_{\xi'}^3 v' &= \sqrt[3]{12}\frac{C_m'}{C_1}\partial_{\xi'}(v' + w'), \\ \partial_{\tau'} w' - 6w'\partial_{\xi'} w' + \partial_{\xi'}^3 w' &= \sqrt[3]{12}\frac{C_m'}{C_2}\partial_{\xi'}(w' + v'), \end{aligned} \tag{8}$$

where we define $\tau' = \tau/2\sqrt{C_1 L_1}$, $\xi' = \sqrt[3]{12}\xi$, $v' = \sqrt[3]{12} m v^{(1)}/6(V_b + V_J)$, and $w' = -\sqrt[3]{12} m w^{(1)}/6(W_b + V_J)$.

At present, a closed-form expression of leapfrogging frequency is evaluated only through approximation for the right-hand side of (8) to be sufficiently small to be treated as perturbative disturbances. As the unperturbed solutions of (8) for v' and w', we consider 1-solitons defined as

$$\begin{aligned} v' &= -2\kappa_1^2 \operatorname{sech}^2 z_1, \\ w' &= -2\kappa_2^2 \operatorname{sech}^2 z_2, \end{aligned} \tag{9}$$

where $z_i = \kappa_i(\xi' - \zeta_i)$ for $i = 1, 2$. Then, the perturbation theory based on the inverse scattering transform predicts the temporal evolutions of κ_i and ζ_i $(i = 1, 2)$ as

$$\begin{aligned} \frac{d\kappa_i}{d\tau'} &= -\frac{\sqrt[3]{12}C_m'}{4C_i\kappa_i}\int_{-\infty}^{\infty} \partial_{\xi'}(v' + w')\operatorname{sech}^2 z_i dz_i, \\ \frac{d\zeta_i}{d\tau'} &= 4\kappa_1^2 - \frac{\sqrt[3]{12}C_m'}{4C_i\kappa_i^3} \\ &\quad \cdot \int_{-\infty}^{\infty} \partial_{\xi'}(v' + w')\operatorname{sech}^2 z_i \left(z_i + \frac{1}{2}\sinh 2z_i\right) dz_i, \end{aligned} \tag{10}$$

where (9) is used for v' and w' [14]. According to [12], leapfrogging is described by the small oscillations of the soliton's amplitudes κ_1 and κ_2 around their average mean values, κ_{01} and κ_{02}, respectively. We then define λ_i as $\kappa_i = \kappa_{0i}(1+\lambda_i)$ for $i = 1, 2$. The variables λ_i are assumed to satisfy the conditions: $\lambda_i \ll 1$. Accordingly, the phase difference $\Delta\zeta \equiv \zeta_1 - \zeta_2$ must be small. We then assume that z_2 is approximately equal to $\kappa_{02}z_1/\kappa_{01} + \kappa_{02}(\lambda_2 - \lambda_1)z_1/\kappa_{01} + \kappa_{02}\Delta\zeta$. Moreover, we define ρ as κ_{02}/κ_{01}. Then, (10) give

$$\frac{d\lambda_1}{d\tau'} = -\frac{\sqrt[3]{12}\alpha(\rho)\rho^2 C_m' \kappa_{02}^2 \Delta\zeta}{C_1}, \tag{11}$$

$$\frac{d\lambda_2}{d\tau'} = \frac{\sqrt[3]{12}\alpha\left(\rho^{-1}\right) C_m' \kappa_{01}^2 \Delta\zeta}{C_2\rho^2}, \tag{12}$$

$$\begin{aligned}\frac{d\zeta_1}{d\tau'} &= 8\kappa_{01}^2\lambda_1 - \frac{\sqrt[3]{12}C_m'\rho^3}{2C_1}\left(3\beta(\rho) + \rho\gamma(\rho)\right)(\lambda_2 - \lambda_1) \\ &\quad + 4\kappa_{01}^2 - \frac{\sqrt[3]{12}C_m'}{2C_1}\left(2 + \rho^3\beta(\rho)\right)\end{aligned} \tag{13}$$

$$\begin{aligned}\frac{d\zeta_2}{d\tau'} &= 8\kappa_{02}^2\lambda_2 \\ &\quad - \frac{\sqrt[3]{12}C_m'\rho^{-3}}{2C_2}\left(3\beta\left(\rho^{-1}\right) + \rho^{-1}\gamma\left(\rho^{-1}\right)\right)(\lambda_1 - \lambda_2) \\ &\quad + 4\kappa_{02}^2 - \frac{\sqrt[3]{12}C_m'}{2C_2}\left(2 + \rho^{-3}\beta\left(\rho^{-1}\right)\right),\end{aligned} \tag{14}$$

where functions α, β, and γ are defined by

$$\begin{aligned}\alpha(x) &= \int_{-\infty}^{\infty} \operatorname{sech}^2 xz\left(1 - 3\tanh^2 xz\right)\operatorname{sech}^2 z\, dz, \\ \beta(x) &= \int_{-\infty}^{\infty} \operatorname{sech}^2 z \operatorname{sech}^2 xz \tanh xz \\ &\quad \cdot (2z + \sinh 2z)\, dz, \\ \gamma(x) &= \int_{-\infty}^{\infty} \operatorname{sech}^2 z \operatorname{sech}^2 xz\left(1 - 3\tanh^2 xz\right) \\ &\quad \cdot z\,(2z + \sinh 2z)\, dz.\end{aligned} \tag{15}$$

By subtracting (14) from (13), $\Delta\zeta$ is shown to satisfy

$$\frac{d^2\Delta\zeta}{d\tau'^2} = -\omega_{\mathrm{lf}}'^2\Delta\zeta, \tag{16}$$

where

$$\begin{aligned}\omega_{\mathrm{lf}}'^2 &= 8\sqrt[3]{18}C_m'\kappa_{01}^4\left(\frac{\alpha\left(\rho^{-1}\right)}{C_2} + \frac{\alpha(\rho)\rho^4}{C_1}\right) \\ &\quad + \sqrt[3]{18}C_m'^2\kappa_{01}^2\left(\frac{\alpha\left(\rho^{-1}\right)}{C_2} + \frac{\alpha(\rho)\rho^6}{C_1}\right) \\ &\quad \times\left(\frac{1}{C_2\rho^6}\left(\gamma\left(\rho^{-1}\right) + 3\beta\left(\rho^{-1}\right)\rho\right)\right. \\ &\quad \left. + \frac{\rho}{C_1}\left(\gamma(\rho)\rho + 3\beta(\rho)\right)\right).\end{aligned} \tag{17}$$

Let the amplitude of a pulse inputted to line i be A_i ($i = 1, 2$), by which κ_{01} and κ_{02} are, respectively, given by $\epsilon^{-1/2}\sqrt{mA_1/(12)^{2/3}(V_b + V_J)}$ and $\epsilon^{-1/2}\sqrt{mA_2/(12)^{2/3}(W_b + V_J)}$. In fact, the voltage fraction A_2/A_1 is expected to be coincident with that of the π mode [15], which becomes L_2/L_1 for small C_m at matched velocities; therefore, ρ becomes coincident with $\sqrt{L_2/L_1}$ in the case of $W_b = V_b$. As a result, once ρ is given, the fraction between C_1 and C_2 is uniquely determined as $C_2 = \rho^{-2}C_1$. Under these assumptions, the angular frequency of leapfrogging is obtained in the units of rad/s as

$$\begin{aligned}\omega_{\mathrm{lf}}^2 &= \frac{m^2\rho^2 C_m A_1^2}{6C_1^2 L_1\left(V_b + V_J\right)^2}\left(\alpha\left(\rho^{-1}\right) + \alpha(\rho)\rho^2\right) \\ &\quad + \frac{m\rho^4 C_m^2 A_1}{8C_1^3 L_1\left(V_b + V_J\right)}\left(\alpha\left(\rho^{-1}\right) + \alpha(\rho)\rho^4\right) \\ &\quad \cdot\left(3\rho^{-1}\beta(\rho) + \gamma(\rho)\right) \\ &\quad + \frac{m\rho^2 C_m^2 A_1}{8C_1^3 L_1\left(V_b + V_J\right)}\left(\alpha(\rho) + \alpha\left(\rho^{-1}\right)\rho^{-4}\right) \\ &\quad \cdot\left(3\rho\beta\left(\rho^{-1}\right) + \gamma\left(\rho^{-1}\right)\right).\end{aligned} \tag{18}$$

In addition, we can evaluate the voltage variation on line 1, denoted as ΔV_1, by solving (16) and substituting the resulting $\Delta\zeta$ into (11):

$$\begin{aligned}\Delta V_1 &= \frac{24\alpha(\rho)\rho^3\Delta x_0\left|A_1\right|}{(18)^{1/3}(12)^{2/3}}\left[\frac{8C_1}{C_m}\left(\alpha\left(\rho^{-1}\right)\right.\right. \\ &\quad \left. + \alpha(\rho)\rho^2\right) + \frac{(12)^{2/3}\left(V_b + V_J\right)}{mA_1}\left(\alpha\left(\rho^{-1}\right)\right. \\ &\quad \left.\left. + \alpha(\rho)\rho^4\right) \times\left(\frac{\gamma\left(\rho^{-1}\right) + 3\beta\left(\rho^{-1}\right)\rho}{\rho^4}\right.\right. \\ &\quad \left.\left. + \rho\left(\gamma(\rho)\rho + 3\beta(\rho)\right)\right)\right]^{-1/2},\end{aligned} \tag{19}$$

Table 1: Line parameter values of coupled NLTLs used to obtain Figure 3.

C_1 (pF)	M	L_1 (nH)	V_J (V)	C_m (pF)	V_b (V)	A_1 (V)	Δx_0 (cell)
1.0	1.0	2.5	1.0	0.01	1.0	2.0	10

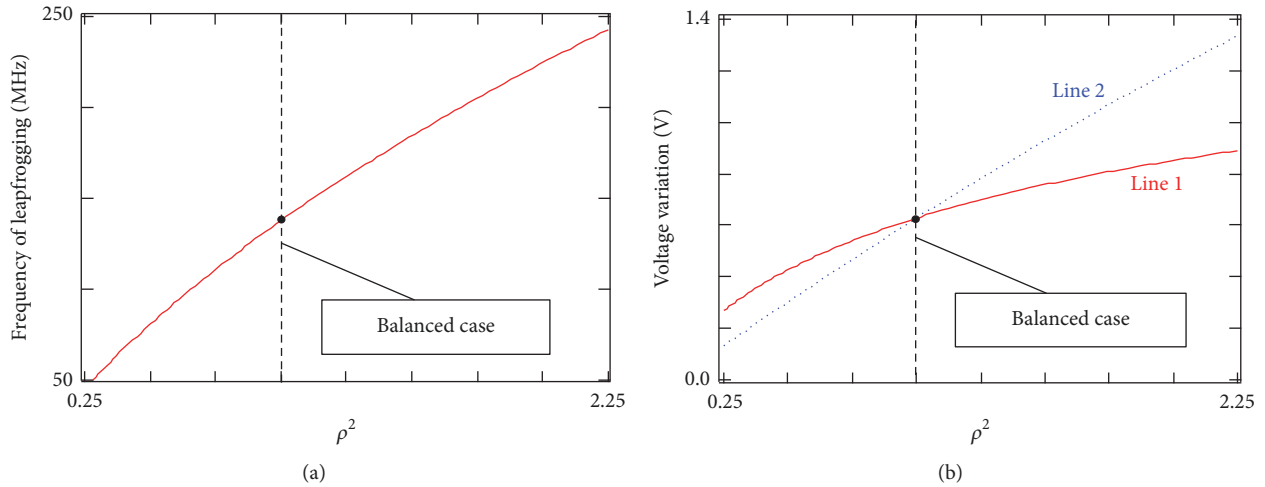

Figure 3: Performance of unbalanced NLTLs obtained by perturbation theory. The dependence of (a) the leapfrogging frequency and (b) voltage variations on ρ.

where Δx_0 represents the initial spatial separation between two pulses in units of *cell*. Similarly, that on line 2 is given by

$$\Delta V_2 = \frac{\alpha\left(\rho^{-1}\right)}{\alpha(\rho)\,\rho^2}\Delta V_1. \tag{20}$$

Figure 3 shows the typical dependence of ω_{lf} and ΔV_i ($i = 1, 2$) on ρ^2 obtained by (18), (19), and (20). The parameter values used to obtain Figure 3 are listed in Table 1. The balanced-line case, corresponding to $\rho = 1.0$, is exemplified by the dashed line. We can see in Figure 3(a) that the leapfrogging frequency increases as ρ becomes large. Because the pulse velocity is only slightly dependent on ρ, the increase in frequency results in the reduction of spatial period of leapfrogging. It is thus expected that the line length for required amplitude modulation can be reduced for larger ρ. The most important result is shown in Figure 3(b), where the voltage variations increase as ρ becomes large. Due to the increase of voltage variations, together with the reduction of required line length, the introduction of imbalance contributes to the effective utilization of leapfrogging pulses in high-speed electrical pulse managements.

3. Numerical Evaluations of Leapfrogging Pulses

In order to examine the leapfrogging pulses in the unbalanced NLTLs, we numerically solved (2) using the fourth-order Runge-Kutta method. For all following calculations, A_1, L_1, C_1, M, V_J, and V_b were set to the values listed in Table 1. In addition, W_b was set equal to V_b. The pulse inputted to line 2 was delayed against that to line 1 by 50 ps. Figure 4 shows the temporal variations of the pulse amplitudes for three different values of ρ, where lines 1 and 2 amplitudes are shown by the thick (blue) and thin (red) curves, respectively. The value of ρ was set to 0.9, 1.0, and 1.5 for Figures 4(a), 4(b), and 4(c), respectively. Note that Figure 4(b) corresponds to the balanced lines. Due to leapfrogging, the pulse on line 1 increases (decreases) when that on line 2 decreases (increases). Because of the instability [16], the leapfrogging period gradually increases in all the calculated cases and the amplitude difference also increases, and thus the spatial separation between leapfrogging pulses gradually increases and finally becomes so large that the interaction is weakened and leapfrogging ceases. The temporal separation between the first and second maximum points of line 2 pulse amplitude, labeled as T_{lf} in Figure 5, is calculated to be 18.5, 16.9, and 13.9 ns for $\rho = 0.9$, 1.0, and 1.5, respectively. The decrease in T_{lf} is qualitatively consistent with the dependence of ω_{lf} on ρ shown in Figure 3(a). The voltage variation between the first peak and bottom of line 2 pulse amplitude is estimated to be 0.37, 0.51, and 1.09 V for $\rho = 0.9$, 1.0, and 1.5, respectively. The calculations successfully validate the prediction that the large ρ results in the increase in amplitude variations.

Finally, we demonstrate the improvement of efficiency in a pulse train modulator by introducing imbalance. Figure 5 shows the result. The line parameter values were those used to obtain Figure 4 except for W_b, which was varied sinusoidally with the frequency of 35 MHz and 0.2 V amplitude around 1.0 V. This variation in W_b affects leapfrogging frequency and amplitude variations of pulses in the NLTLs, resulting in the modulated pulse train at the output. The pulse with the width of about 60 ps was repeatedly applied to the inputs with the period of 2 ns. The total cell size was 210. Figure 5(a) shows the temporal waveform recorded at the output for the balanced NLTLs. Sinusoidal modulation is established for the

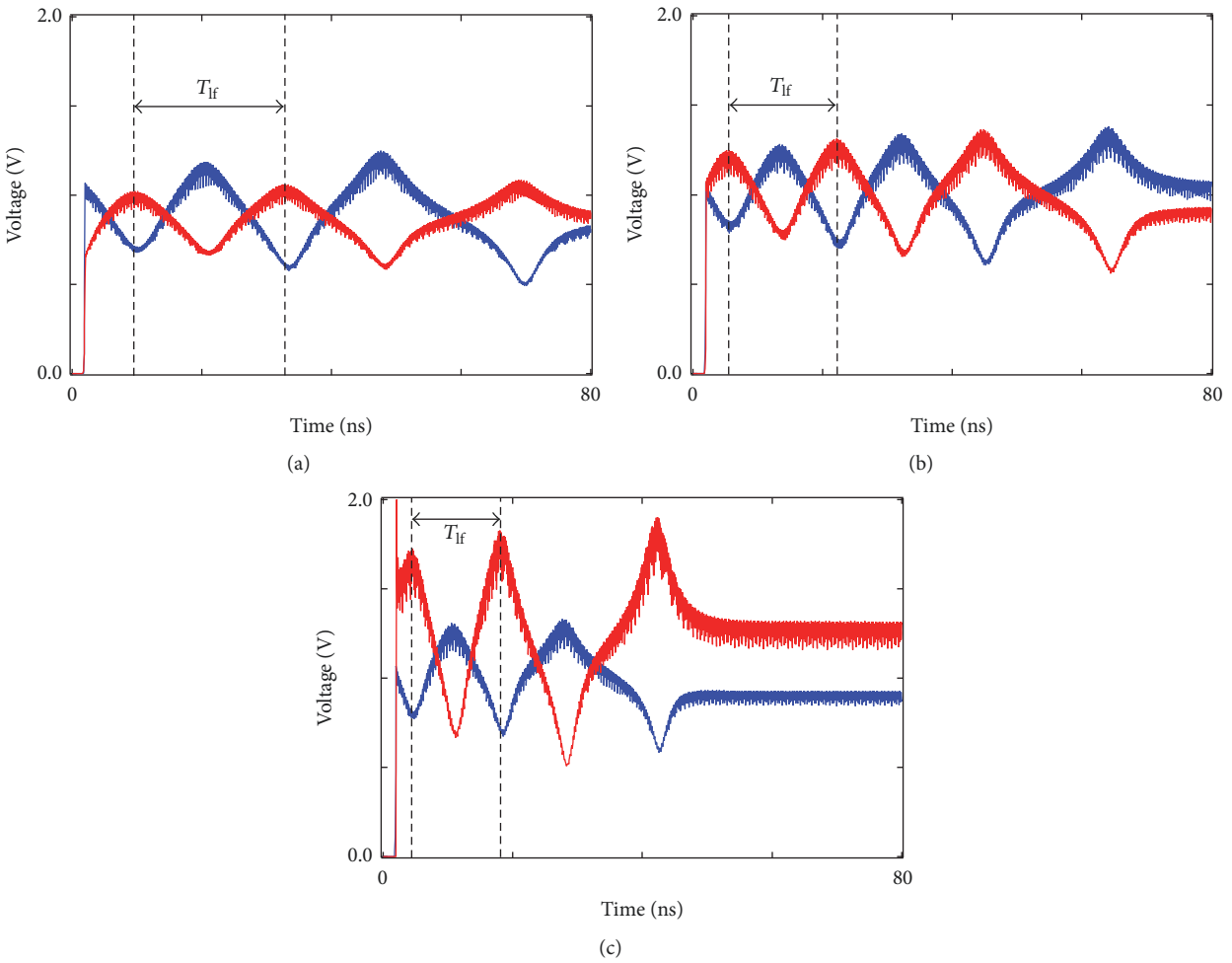

Figure 4: Amplitude variation of leapfrogging pulses. The cases corresponding to three different values of ρ were examined [(a) $\rho = 0.9$, (b) $\rho = 1.0$, and (c) $\rho = 1.5$].

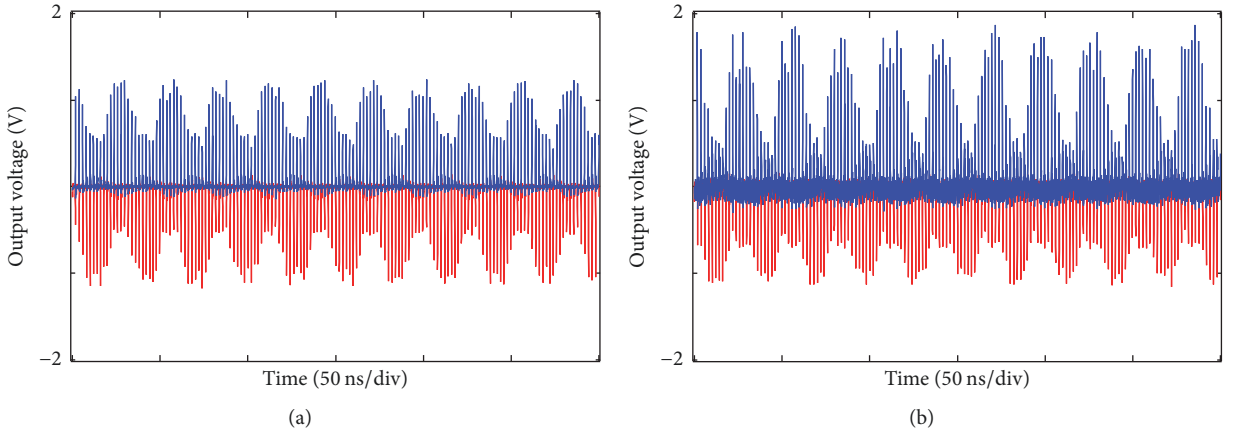

Figure 5: Improvement of modulation efficiency using unbalanced NLTLs.

outputted pulse train. However, the on/off ratio is about 2.0 at most for both line outputs. On the other hand, Figure 5(b) shows the output waveforms for $\rho = 1.5$. Although the on/off ratio becomes deteriorated at the line 1 output, it is significantly improved to be beyond 4.0 at the output of line 2. Note that the modulated amplitude of V_{out} is significantly greater than V_{mod} amplitude. It seems possible to reduce the line length required for sufficient on/off ratio of modulated pulse train by further optimization of line parameter values and biasing conditions.

4. Conclusions

The properties of leapfrogging pulses in two coupled NLTLs, which share a common wave velocity and possess their own characteristic impedances, are investigated. The common wave velocity guarantees the resonance interaction between pulses traveling in the lines. We investigated the impact of line imbalance resulting from the different characteristic impedance on the leapfrogging pulses to show that both the leapfrogging frequency and voltage variations increase, based on the analysis using the soliton perturbation theory. Several numerical calculations validate these observations and successfully demonstrate the improved performance of pulse train modulation using leapfrogging pulses.

Conflicts of Interest

The author declares that there are no conflicts of interest regarding the publication of this paper.

References

[1] J. A. Gear and R. Grimshaw, "Weak and strong interactions between internal solitary waves," *Studies in Applied Mathematics*, vol. 70, no. 3, pp. 235–258, 1984.

[2] S. Y. Lou, B. Tong, H.-c. Hu, and X.-y. Tang, "Coupled KdV equations derived from two-layer fluids," *Journal of Physics A: Mathematical and General*, vol. 39, no. 3, pp. 513–527, 2006.

[3] A. K. Liu, T. Kubota, and D. R. Ko, "Resonant transfer of energy between nonlinear waves in neighboring pycnoclines," *Studies in Applied Mathematics*, vol. 63, no. 1, pp. 25–45, 1980.

[4] A. K. Liu, N. R. Pereira, and D. R. Ko, "Weakly interacting internal solitary waves in neighbouring pycnoclines," *Journal of Fluid Mechanics*, vol. 122, pp. 187–194, 1982.

[5] P. D. Weidman and M. Johnson, "Experiments on leapfrogging internal solitary waves," *Journal of Fluid Mechanics*, vol. 122, pp. 195–213, 1982.

[6] M. Nitsche, P. D. Weidman, R. Grimshaw, M. Ghrist, and B. Fornberg, "Evolution of solitary waves in a two-pycnocline system," *Journal of Fluid Mechanics*, vol. 642, pp. 235–277, 2010.

[7] K. Narahara, "Characterization of leapfrogging solitary waves in coupled nonlinear transmission lines," *Nonlinear Dynamics*, vol. 81, no. 4, pp. 1805–1814, 2015.

[8] M. J. W. Rodwell, S. T. Allen, U. Bhattacharya et al., "Active and nonlinear wave propagation devices in ultrafast electronics and optoelectronics," *IEEE*, vol. 82, no. 7, pp. 1037–1059, 1994.

[9] M. Kintis, X. Lan, F. Fong et al., "An MMIC pulse generator using dual nonlinear transmission lines," *IEEE Microwave and Wireless Components Letters*, vol. 17, no. 6, pp. 454–456, 2007.

[10] K. Narahara, "Characterization of nonlinear transmission lines for short pulse amplification," *Journal of Infrared, Millimeter, and Terahertz Waves*, vol. 31, no. 4, pp. 411–421, 2010.

[11] A. Jeffrey and T. Kawahara, *Asymptotic Methods in Nonlinear Wave Theory*, Pitman, London, UK, 1982.

[12] B. A. Malomed, ""Leapfrogging" solitons in a system of coupled KdV equations," *Wave Motion*, vol. 9, no. 5, pp. 401–411, 1987.

[13] Y. S. Kivshar and B. A. Malomed, "Solitons in a system of coupled Korteweg-de Vries equations," *Wave Motion*, vol. 11, no. 3, pp. 261–269, 1989.

[14] Y. S. Kivshar and B. A. Malomed, "Dynamics of solitons in nearly integrable systems," *Reviews of Modern Physics*, vol. 61, no. 4, pp. 763–915, 1989.

[15] R. Garg, I. Bahl, and M. Bozzi, *Microstrip Lines and Slotlines*, Artech House, Boston, Mass, USA, 2013.

[16] J. D. Wright and A. Scheel, "Solitary waves and their linear stability in weakly coupled KdV equations," *Zeitschrift für Angewandte Mathematik und Physik*, vol. 58, no. 4, pp. 535–570, 2007.